Desalination and Water Treatment
www.deswater.com
doi: 10.1080/19443994.2014.899519

54 (2015) 2432–2440
May

Taylor & Francis
Taylor & Francis Group

Synthesis, treatment, and application of a novel carbon nanostructure for removal of fluoride from aqueous solution

Hossein Faghihian[a,*], Homa Atarodi[b], Masoume Kooravand[b]

[a]*Department of Chemistry, Shahreza Branch, Islamic Azad University, Shahreza, Iran, Tel. +983213213095; email: Faghihian@iaush.ac.ir*
[b]*Young Researchers Club, Shahreza Branch, Islamic Azad University, Shahreza, Iran*

Received 12 August 2013; Accepted 21 February 2014

ABSTRACT

In this research, a new carbon nanostructure was prepared by chemical vapor deposition method on the surface of kaolin disks. Cyclohexanol and ferrocene were respectively used as carbon source and catalyst. In order to enhance the adsorption capacity of carbon nanostructure for fluoride adsorption, the disks were treated with 1 M KOH at reflux conditions. The scanning electron microscopy image showed that "sword like" nanostructures with 70 nm in diameter and 7030 nm in length were formed on the surface of kaolin. The Infrared spectra of the treated sample revealed that the hydroxyl and carboxyl groups were produced on the surfaces. The surface functional groups were determined by the Boehm titration. Adsorption experiments indicated that removal of fluoride by the treated sample was pH dependant and under optimized condition 230.61 meq/g of F^- was adsorbed, which was beyond of the capacity of the earlier studied adsorbents.

Keywords: Chemical vapor deposition; Carbon nanostructures; Adsorption; Fluoride; Surface treatment; Boehm's titration; $pH_{(PZC)}$

1. Introduction

Carbon nanotubes (CNTs) are a relatively new class of synthesized carbonaceous materials and are considered to be promising candidates for many areas of applications including special adsorbents in water treatment and environmental remediation. CNTs have large surface area, high mechanical strength, and remarkable electrical conductivities, which have been indicate for their tremendous potential for different applications [1,2]. Synthesis of the CNTs via chemical vapor deposition method has shown to be more controllable and cost-efficient when compared with other synthetic high temperature methods such as arc discharge [3] or laser vaporization [4]. The oxidation of CNTs either by wet chemical methods [5–8], photo-oxidation [9,10], oxygen plasma [11], or gas phase treatment [12] has gained a lot of attention in an attempt to purify and to enhance the chemical reactivity of the graphitic network. Oxygen-containing functional groups (OH, C=O, and COOH) can be introduced on carbon nanostructures through liquid-phase oxidation procedures [13].

The acceptable fluoride concentration in drinking water is generally in the range 0.5–1.5 mg/L [14]. Concentration higher than that will affect the metabolism of elements such as Ca and P in human body

*Corresponding author.

and lead to dental and bone fluorosis [15]. Many methods have been developed for fluoride removal from water, including adsorption [16], ion exchange, electro dialysis [17], and precipitation [18]. Among these methods, adsorption is a widely used method for defluorination [19]. Recently, Long et al. reported that carbon nanotube had better adsorption capacity for dioxin removal than that of activated carbon [20]. Li et al. suggested that CNTs had high efficiency for Pb^{2+}, Cd^{2+}, and F^{-} removal from aqueous solution after oxidation treatment [21–23]. In this work, a new carbon nanostructure was synthesized by chemical vapor deposition method on macroporous kaolin substrate surface by using cyclohexanol and ferrocene as carbon source and catalyst, respectively. In order to increase the adsorption capacity of the nanostructures toward fluorine, it was modified with KOH. The effect of different parameters on the adsorption capacity was studied and optimized.

2. Experimental

The small disks of kaolin (2.5 cm diameter, 10 mm thickness) were prepared by compressing kaolin paste in special molds. The disks were dried at 120˚C for 24 h followed by calcinations at 800˚C for 3 h and then were polished with 800 and 1,000 mesh sand papers and cleaned in an ultrasonic acetone bath for 30 min. The kaolin disks were placed horizontally in the middle of a CVD reactor. A schematic diagram of the experimental set-up is shown in Fig. 1. The CVD reactor consisted of a horizontal stainless steel tube (70 cm long, inner diameter of 3.2 cm) that was housed in a cylindrical furnace. This reactor had two inlet paths: one for carrier gas (nitrogen) and the other for the reagent. A flask containing 10 mL of cyclohexanol as carbon source and 0.5 g of ferrocene as catalyst was connected to the reactor nearby the carrier gas inlet.

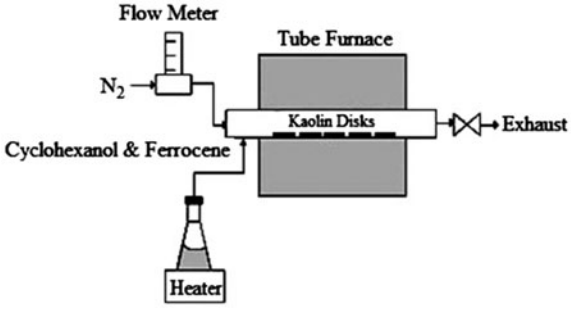

Fig. 1. Schematic diagram of the CVD reactor.

At first, the reactor was purged with nitrogen in order to eliminate oxygen from the reaction chamber. The reactor was preheated to 750˚C subsequently, the flask containing the carbon source and catalyst was placed in an oil bath (at 200˚C) for immediate vaporization of the reagents. The vapors were carried to the furnace by nitrogen flow. After 90 min, the furnace was switched off and the reactor was cooled gradually to room temperature under nitrogen flow and the disks were removed [24]. The chemical treatment of the synthesized materials was carried out with KOH (1 M) at reflux conditions for 3 h [25]. The treated carbon nanostructures were subsequently washed with distilled water until neutral pH and dried in a vacuum-oven at 90˚C for 12 h. The surface functional groups were measured according to the Boehm's titration method. To three vials containing 25 mL of 0.1 N of sodium hydroxide, sodium carbonate, or sodium bicarbonate, 0.02 g of CNS was added. The vials were sealed and shaken for 24 h, and then, the solid was separated by filtration. Ten milliliter of the filtrate was pipetted, and the excess base was titrated with HCl (0.1 N). The number of acidic sites was determined by the assumption that NaOH neutralizes carboxylic, lactonic, and phenolic groups; Na_2CO_3 neutralizes carboxylic and lactonic groups; and $NaHCO_3$ neutralizes only carboxylic groups [26]. The pH where the net total particle charge is zero is called the point of zero charge (PZC), which is one of the most important parameters used to describe variable-charge surfaces. The pH drift test was carried out as follows: 25 mL of 0.01 M NaCl solution was placed in a vessel at 298 K and nitrogen was bubbled through the solution to stabilize the pH by preventing the dissolution of CO_2. The pH was adjusted to a value between 1 and 9 by addition of 0.1 M HCl or 0.1 M NaOH solution. 0.02 g of CNS was added to the solution and after 3 h the final pH was measured. The measured values were plotted against the initial pH. The pH at which the curve crossed the line $pH_{initial} = pH_{final}$ was taken as the PZC, pH_{pzc} [27]. The fluoride solution (3,000 ppm) was prepared by dissolving of NaF in deionized water. The adsorption experiments were carried out in polyethylene tubes at room temperature by putting 0.02 g of CNS in contact with 40 mL of NaF solution. After the pH was adjusted with HNO_3 or NaOH solution, the tubes were shaken for 24 h. The solution was filtered and the fluoride concentration was measured by a fluoride ion-selective electrode. The amount of fluoride adsorbed on the nanostructure was determined as the difference between initial and final concentration.

3. Results and discussion

In different parts of the SEM images, "sword like" nanostructures (about 70 nm in diameter and lengths of a few hundred nm were observed on the surface of kaolin (Fig. 2). The formation of different nanostructure compounds and this structure has already been reported [24,28].

On the FT-IR spectra of the treated sample, the presence of oxygen-containing functional groups was clearly observed (Fig. 3).

In the FT-IR spectra of kaolin, Fig. 3(a), the characteristic adsorption bands of kaolin including Si–O and Si–O–Si elongation vibrations at 1,079–1,086 cm^{-1} were observed. The bands at 800–815 and 477–480 cm^{-1} attributed to Al–O–H and Si–O–Al vibrations were also detected [29,30]. In the FT-IR of carbon nanostructures, Fig. 3(b), the band at 1,631 cm^{-1} attributed to C=C stretching was observed while the C–H stretching band at 2,800–3,000 cm^{-1} was not detected indicating that the carbon source; cyclohexanol was decomposed during the course of the synthesis. In the FT-IR of the treated CNS, besides the adsorption bands of the substrate, a new band at 1,650 cm^{-1} attributed to stretching vibrations of carbonyl groups (C=O) of carboxylic acids (–COOH) was appeared Fig. 3(c). The wide band at 3,426 cm^{-1} attributed to O–H stretching was also observed. Various adsorbents including carbon nanostructures can absorb moisture, so the peak observed at 3,435 cm^{-1} attributed to OH stretching of water molecules. After treatment with KOH, the wide peak observed at 3,426 cm^{-1}. More strain and more broadening of this peak indicated that the hydroxyl group with a hydrogen bond was formed as indicated in Fig. 4, [13,31]. The C=C band at 1,631 was overlapped with the carboxylic groups.

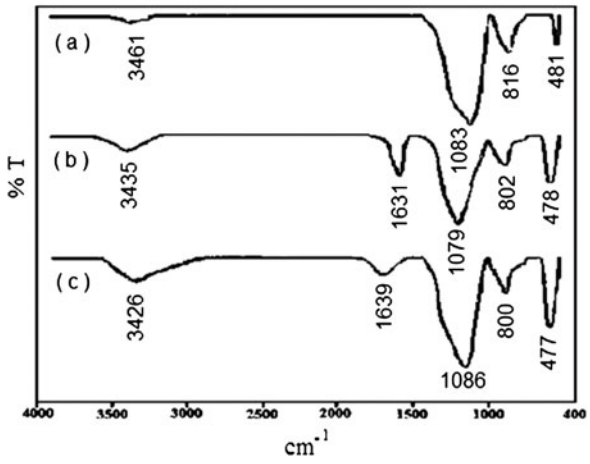

Fig. 3. Infrared spectra of kaolin disk (a), disk with nanostructure (b), and disk after treatment (c).

The result of Boehm titration for the synthesized CNS and treated CNS is given in Table 1. It was evident that the presence of functional groups was significantly increased after treatment. According to the earlier researches, after acid treatment, due to the presence of carboxylic sites, the $pH_{(PZC)}$ of the sample was shifted to lower pH [23,32]. In this work, the $pH_{(PZC)}$ was shifted to higher pH ($pH_{pzc} = 5.37$) (Fig. 5). It is suggested that under the experimental conditions of this research more hydroxyl groups were formed rather than carboxylic groups.

In the adsorption experiments, the chemical interaction between the anions and the surface functional groups of carbon nanostructures is the major mechanism of the sorption. The pH value at which the zeta potential equals to zero is called PZC, and it is used to assess the adsorbent surface charge qualitatively [19]. When the pH of the solution is lower than the pH_{PZC} of the adsorbent, the positive charge on the surface provides electrostatic attractions that are favorable for adsorbing anions. The increase in pH leads to the neutralization of surface charge, so the adsorption of anions on to nanostructure was quickly decreased. The adsorption isotherm of fluoride by treated carbon nanostructures at different pH values is given in Figs. 6 and 7. The significant decrease in fluoride adsorption capacity at pH 1 was attributed to the structural change of CNS, which resulted in separation of functional groups [33,34]. At pH 2, the surface became positive and the highest protonation of the surface occurred; therefore, the maximum adsorption capacity was obtained at this pH. As the pH raised to

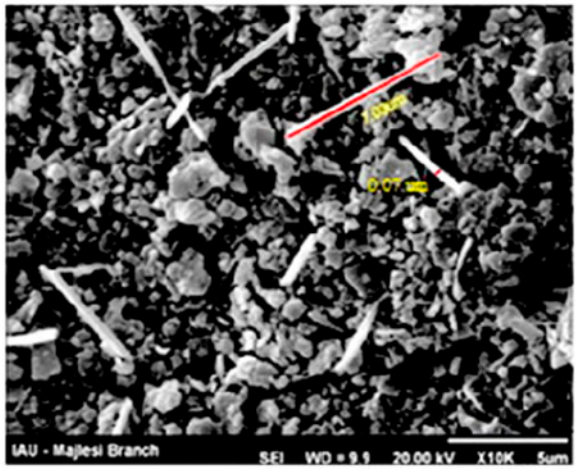

Fig. 2. SEM image of carbon nanostructure.

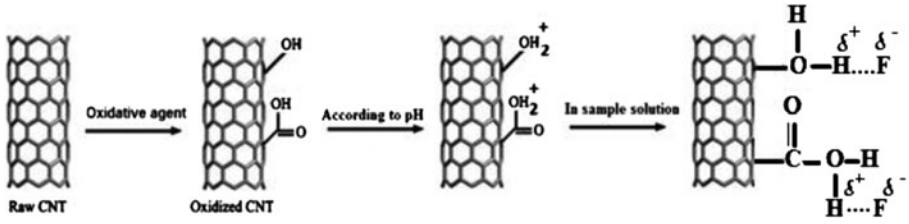

Fig. 4. Adsorption of fluoride on the surface of the treated nanotube.

Table 1
The results of Boehm titration

Sample	Carboxylic sites (mmol/g)	Phenolic sites (mmol/g)	Lactonic sites (mmol/g)	$pH_{(PZC)}$
Non-treated	0.42	1.08	0.71	5.37
Treated	1.50	7.00	8.50	6.02

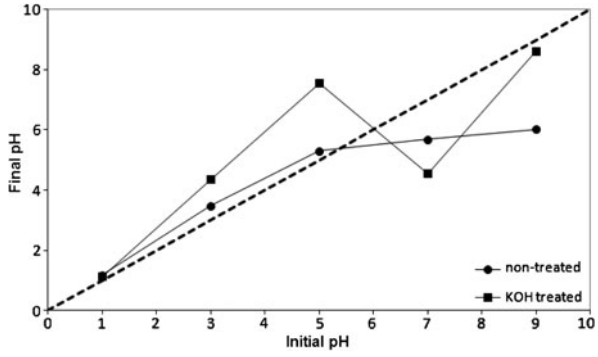

Fig. 5. The $pH_{(PZC)}$ of the carbon samples using the pH drift method.

the $pH_{(PZC)}$ value, the adsorption of anion decreased. At higher pHs the competition between OH^- and F^- for active sites and the negative charge of the surface on the other hand lower adsorption capacity. At pH 7, the lowest capacity of 8.54 meq/g was obtained [19].

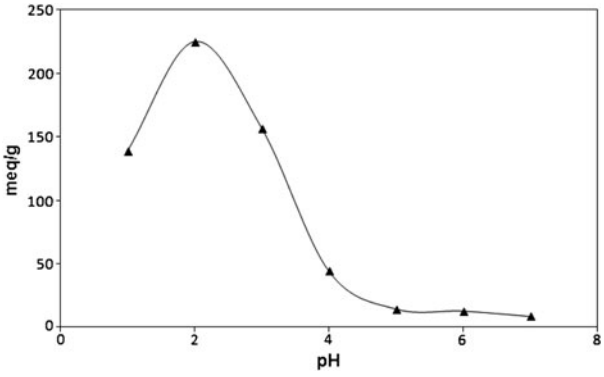

Fig. 6. Effect of contacting pH on adsorption of F^- ($V_0 = 40$ mL, $C_0 = 3{,}000$ mg/L, adsorbent dosage = 0.02 g).

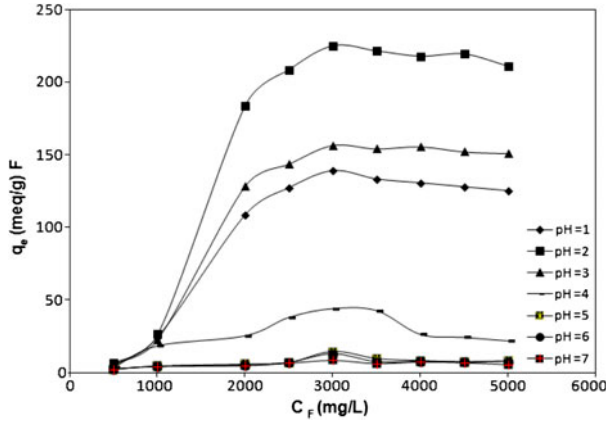

Fig. 7. Adsorption isotherms of treated carbon nanostructures at 25°C.

With increasing the initial concentration, the fluoride adsorption significantly increased (Fig. 7). The adsorption onto the treated carbon nanostructures is a diffusion-based process; therefore, with increasing initial concentration, the anion diffused more rapidly into the cavities of the adsorbent. The optimized adsorption capacity of the synthesized nanostructure was much higher than those reported earlier for similar adsorbents. Li et al. reported adsorption capacity of 1.22 meq/g at pH 2 for activated carbon [19]. Eom et al. obtained very low capacity for aligned CNTs at pH 7 [35]. Li et al. reported that the monolayer adsorption capacity of fluoride by graphene was 1.87

meq/g at pH 7 [36]. In this study, the adsorption capacity of 230.61 meq/g for the sample treated with KOH was obtained, which was higher than the reported values.

Fig. 8 shows the effect of contacting time on the adsorption of fluoride onto treated carbon nanostructures. It was observed that the adsorption of F^- increased rapidly with time and after 4 h the equilibration was established, and the maximal capacity was observed.

To study the adsorption kinetic, three models, namely pseudo-first-order, pseudo-second-order, and intra-particle diffusion models, were analyzed. The pseudo-first-order equation is expressed as follows [37]:

$$\log\ (q_e - q_t) = \log\ q_e - (k_1/2.303)t \quad (1)$$

where k_1 is the Lagergren rate constant of adsorption (1/min). The plot of log $(q_e - q_t)$ against t gives a linear relationship from which k_1 and q_e are determined from the slope and intercept of plot, respectively.

The pseudo-second-order model can be represented by the following linear form [38]:

$$t/q_t = 1/k_2 q_e^2 + (1/q_e)t \quad (2)$$

where k_2 is the pseudo-second-order rate constant of adsorption (g/mg min). The values of q_e and k_2 are determined from the slope and intercept of the plot of t/q_t against t.

The validity of each kinetic model was checked by the fitted straight shown in Figs. 9 and 10. The corresponding kinetic parameters are summarized in Table 2.

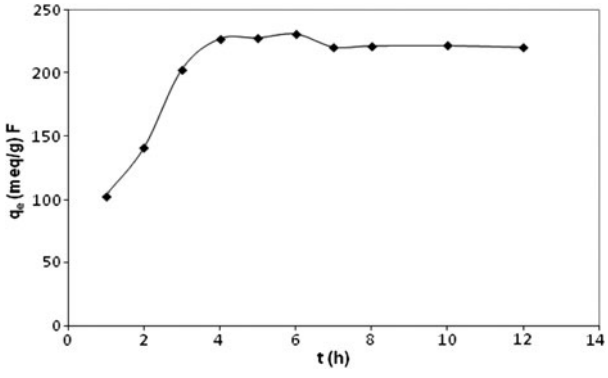

Fig. 8. Effect of contacting time on the adsorption of F^- (V_0 = 40 mL, C_0 = 3,000 mg/L, pH 2.0, adsorbent dosage = 0.02 g).

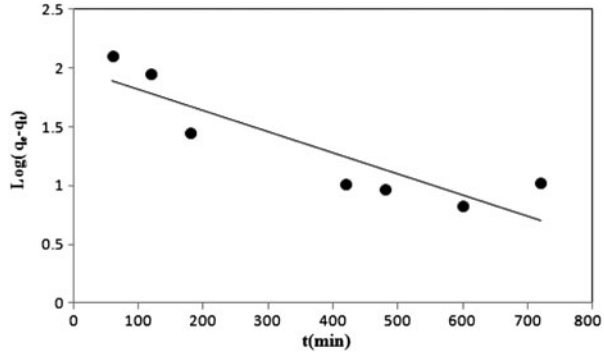

Fig. 9. Pseudo-first-order kinetic model of fluoride adsorption by treated CNS.

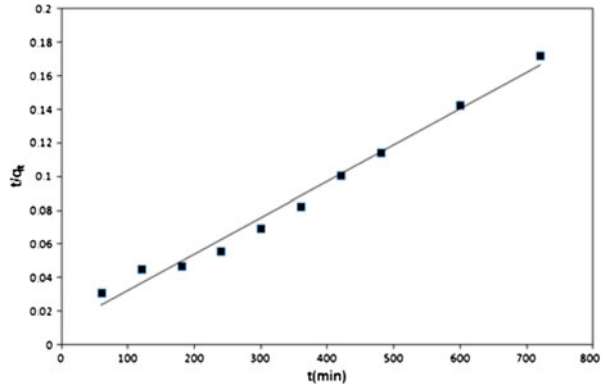

Fig. 10. Pseudo-second order kinetic model of fluoride adsorption by treated CNS.

The intra-particle diffusion model is expressed by followed equation [39]:

$$q_t = k_p t^{1/2} + C \quad (3)$$

Besides the adsorption at the outer surface of the adsorbent, the adsorbate molecules may also diffuse into the interior of the porous adsorbent. This was studied by plotting the amount of fluoride adsorbed

Table 2
Kinetics parameters for adsorption of fluoride onto treated carbon nanostructures at 25℃

Intra-particle diffusion		Pseudo-second order		Pseudo-first order	
R^2	C	R^2	$K_2 \times 10^{-6}$	R^2	K_1
0.5840	102.7	0.9478	3.7	0.8008	4.1×10^{-3}

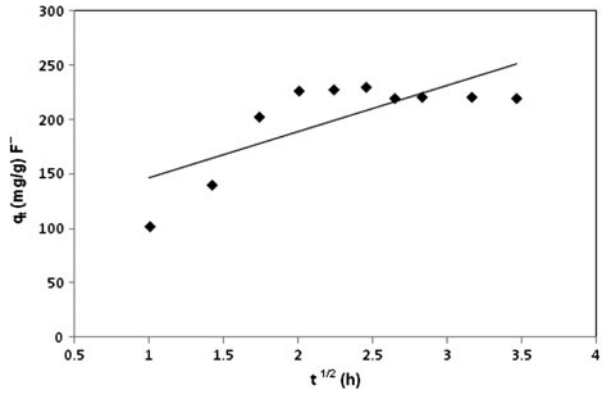

Fig. 11. Intraparticle diffusion for adsorption of fluoride.

vs. the square root of time for different initial fluoride concentrations (Fig. 11). From Table 2, the results indicating that the experimental data are well described by pseudo-second-order model and the nature of adsorption is a chemical-controlling process. Mechanism of the adsorption of fluoride on the surface of treated carbon nanotube can be suggested as depicted in (Fig. 4) [31].

The effect of temperature on the removal of fluoride by treated carbon nanostructures was investigated at four different temperatures 25, 35, 45, and 55°C (Fig. 12). It was concluded that the fluoride adsorption increased with the rise of temperatures. With increasing the temperature, the mobility of small ions of fluoride increased and the effective collision between the anion and the surface of adsorbent increased. Similar observation was made by Satish et al. [40]. They observed that as the experimental temperature increased from 298 to 318 K, the fluoride ion adsorption increased for most of the studied adsorbents indicating that the sorption process was endothermic in nature.

Thermodynamic parameters of adsorption, standard free energy change (ΔG°), standard enthalpy change (ΔH°), and standard entropy change (ΔS°) were calculated using the following equations:

$$\Delta G^\circ = -RT \ln K_0 \tag{4}$$

where (ΔG°) is standard free energy change of sorption (kJ/mol), T is the temperature in Kelvin, and R is universal gas constant (8.314 J/mol/K) and K_0 is the sorption equilibrium constant. The standard enthalpy change (ΔH°) and standard entropy change (ΔS°) were calculated using the Vant Hoof equation [36]:

$$\ln K_0 = (-\Delta H^\circ/RT) + \Delta S^\circ/RT \tag{5}$$

where (ΔH°) is standard enthalpy change (kJ/mol), and (ΔS°) is standard entropy change (kJ/mol K). The values of (ΔH°) and (ΔS°) were obtained from the slope and intercept of ln K_0 against $1/T$ (Fig. 13). The values of K_0, ΔG°, ΔH°, and ΔS° are given in Table 3.

The negative value of standard free energy change and positive value of entropy change indicated that fluoride adsorption was a spontaneous reaction. The positive value of enthalpy change indicated that the reaction is endothermic.

Adsorption isotherms can be generated based on numerous theoretical models, where Langmuir and Freundlich models are the most frequently used. The Freundlich model is an empirical equation based on adsorption on a heterogeneous surface [36]. The Freundlich isotherm model can be expressed in a linear form:

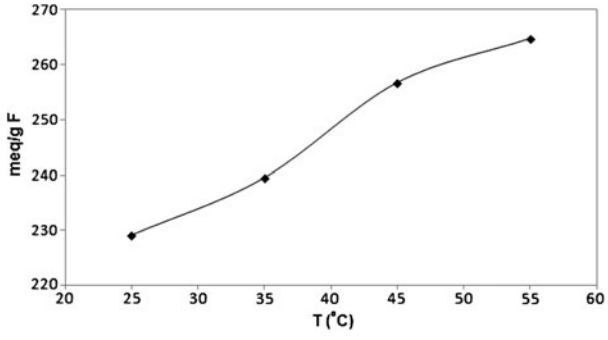

Fig. 12. Effect of temperature on adsorption ($V_0 = 40$ mL, $C_0 = 3{,}000$ mg/L, contacting time = 4 h, pH 2.0, adsorbent dosage = 0.02 g).

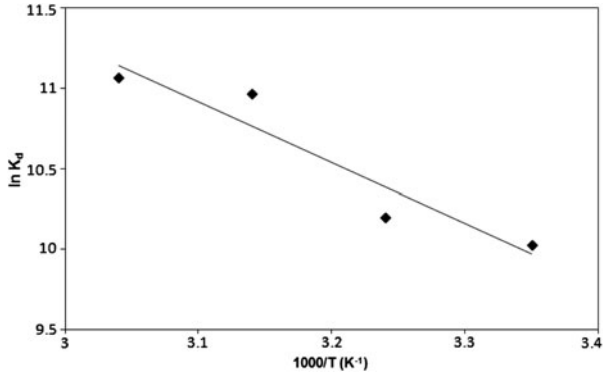

Fig. 13. Plot of ln K_d vs. $(1/T)$ for adsorption of fluoride.

Table 3
Thermodynamic parameters for adsorption of fluoride onto treated carbon nanostructures

	ΔG° (J/mol)					
R^2	55℃	45℃	35℃	25℃	ΔS° (J/mol K)	ΔH° (J/mol)
0.8977	−61570.38	−59692.28	−57814.18	−55936.08	187.81	31.30

$$\log q_e = 1/n \log C_e + \log K_F \quad (6)$$

Here, K_F and n are Freundlich constants, related to adsorption capacity and adsorption intensity (heterogeneity factor), respectively. For $n = 1$, the partition between the two phases is independent of the concentration. The situation $n < 1$ is the most common and corresponds to a normal Langmuir isotherm, while $n > 1$ is indicative of a cooperative sorption, which involves strong interactions between the molecules of adsorbents.

The values of K_F and $1/n$ were obtained from the slope and intercept of the linear Freundlich plot of log q_e vs. log C_e shown in Fig. 14.

The Langmuir model supposes that uptake of the species occurs on a homogenous surface by monolayer adsorption without any interaction between adsorbed compounds, with homogeneous binding sites, equivalent sorption energies, and no interaction between adsorbed species. The equation of the Langmuir adsorption model can be expressed in a linear form:

$$C_e/q_e = 1/q_m K_L + C_e(1/q_m) \quad (7)$$

where q_e is the equilibrium adsorption, in mg/g, C_e is the equilibrium concentration of fluoride, in mg/L, q_m is the maximum adsorption capacity corresponding to the complete monolayer coverage, in mg/g, and K_L is the Langmuir constant, which is related to the energy of adsorption. The values of Langmuir parameters q_m and K were calculated from the slope and intercept of the linear plots of $1/q_e$ vs. $1/C_e$ shown in Fig. 15.

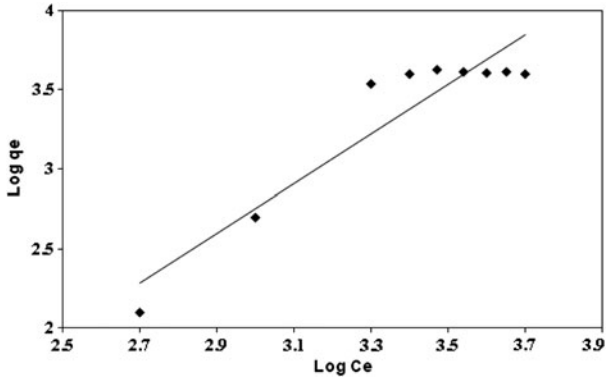

Fig. 14. Freundlich isotherm model at 25℃ for fluoride adsorption.

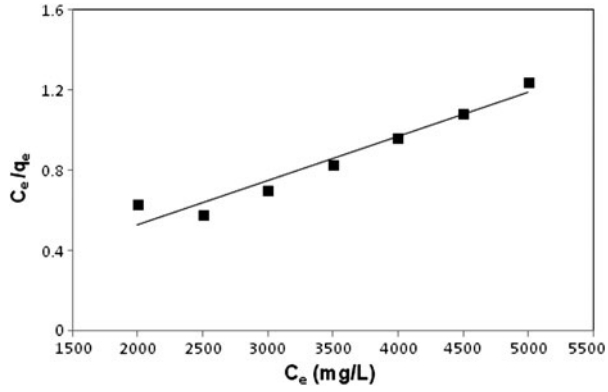

Fig. 15. Langmuir isotherm model at 25℃ for fluoride adsorption.

In order to predict the adsorption efficiency of the process, the dimensionless quantity (R_L) was calculated by using the equation:

$$R_L = 1/(1 + K_L C_0) \quad (8)$$

where C_0 and K_L are the initial concentration of fluoride and Langmuir isotherm constant. If the value of $R_L < 1$, it represents favorable adsorption and greater than 1.0 represents unfavorable adsorption. The values of Langmuir and Freundlich constants are given in Table 4. From this table, higher correlation coefficients indicated that the Langmuir model fits the adsorption data better than the Freundlich model.

4. Regeneration of the adsorbent

To regenerate the used adsorbent, two different solutions were separately examined; NaOH 1 M and HNO_3 1 M. At optimized conditions, full original capacity was obtained for the sample washed with NaOH while for the sample washed with HNO_3 only

Table 4
Isotherms parameters for fluoride adsorption by treated CNS with KOH

	Langmuir isotherm			Freundlich isotherm		
Adsorbent	R^2	R_L	q_m	R^2	K_F	n
Treated CNS	0.94	0.14	5,000	0.87	0.011	0.63

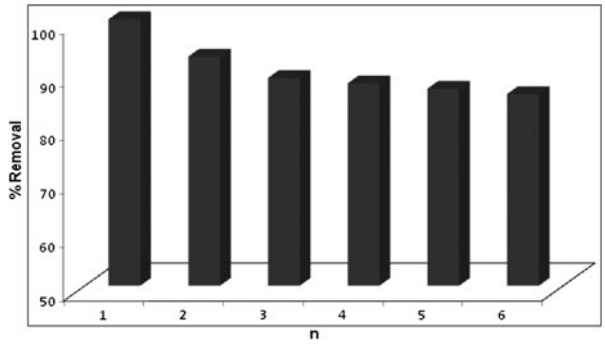

Fig. 16. Sorption–desorption study of F^- with treated carbon nanostructures.

46% of the original capacity was recovered. The adsorption–regeneration process was repeated for six successive cycles with NaOH. It was concluded that more than 85% of the capacity was recovered after the last regeneration step (Fig. 16).

5. Conclusion

The results of this study showed that the carbon nanostructure treated with KOH was an effective adsorbent for removal of fluoride from aqueous solution with the highest adsorption capacity ever reported. The experimental data were well fitted with the Langmuir isotherm equation. After treatment with KOH, new oxygen-containing functional groups were formed on the surface of the adsorbent that enhanced the adsorption capacity toward fluoride ions; therefore, the adsorption capacity of 230.61 meq/g was obtained. Thermodynamic studies showed that the process was spontaneous and endothermic. Kinetic data were well fitted to a pseudo-second-order kinetic model, suggesting that the adsorption was a chemical-controlling process. The experimental data fitted with the Langmuir isotherm equation also confirmed the monolayer adsorption, which showed the chemical nature of the adsorption.

References

[1] S. Iijima, Helical microtubules of graphitic carbon, Nature 354 (1991) 56–58.
[2] P. Ganesan, R. Kamaraj, G. Sozhan, S. Vasudevan, Oxidized multiwalled carbon nanotubes as adsorbent for the removal of manganese from aqueous solution, Environ. Sci. Pollut. Res. 20 (2013) 987–996.
[3] T.W. Ebbesen, P.M. Ajayan, Large-scale synthesis of carbon nanotubes, Nature 358 (1992) 220–222.
[4] A. Thess, R. Lee, P. Nikolaev, H. Dai, P. Petit, J. Robert, C. Xu, Y.H. Lee, S.G. Kim, A.G. Rizler, D.T. Colbert, G.E. Scuseria, D. Tomanek, J.E. Fischer, R.E. Smalley, Crystalline ropes of metallic carbon nanotubes, Science 273 (1996) 483–487.
[5] J. Chen, M.A. Hamon, H. Hu, Y. Chen, A.M. Rao, P.C. Eklund, R.C. Haddon, Solution properties of single-walled carbon nanotubes, Science 282 (1998) 95–98.
[6] K.J. Ziegler, Z. Gu, H. Peng, E.L. Flor, R.H. Hauge, R.E. Smalley, Controlled oxidative cutting of single-walled carbon nanotubes, J. Am. Chem. Soc. 127 (2005) 1541–1547.
[7] J. Zhang, H. Zou, Q. Qing, Y. Yang, Q. Li, Z. Liu, X. Guo, Z. Du, Effect of chemical oxidation on the structure of single-walled carbon nanotubes, J. Phys. Chem. B 107 (2003) 3712–3718.
[8] I.D. Rosca, F. Watari, M. Uo, T. Akasaka, Oxidation of multiwalled carbon nanotubes by nitric acid, Carbon 43 (2005) 3124–3131.
[9] M. Grujicic, G. Cao, A.M. Rao, T.M. Tritt, S. Nayak, UV-light enhanced oxidation of carbon nanotubes, Appl. Surf. Sci. 214 (2003) 289–303.
[10] T. Savage, S. Bhattacharya, B. Sadanadan, J. Gaillard, T.M. Tritt, Y.P. Sun, Y. Wu, S. Nayak, R. Car, N. Marzari, P.M. Ajayan, A.M. Rao, Photoinduced oxidation of carbon nanotubes, J. Phys. Condens. Matter 15 (2003) 5915–5921.
[11] A. Felten, C. Bittencourt, J.J. Pireaux, Gold clusters on oxygen plasma functionalized carbon nanotubes: XPS and TEM studies, Nanotechnology 17 (2006) 1954–1959.
[12] S.C. Tsang, P.J.F. Harris, M.L.H. Green, Thinning and opening of carbon nanotubes by oxidation using carbon dioxide, Nature 362 (1993) 520–522.
[13] F. Avilés, J.V. Cauich-Rodríguez, L. Moo-Tah, A. May-Pat, R. Vargas-Coronado, Evaluation of mild acid oxidation treatments for MWCNT functionalization, Carbon 47 (2009) 2970–2975.
[14] M. Hichour, F. Persin, J. Molénat, J. Sandeaux, C. Gavach, Fluoride removal from diluted solutions by Donnan dialysis with anion-exchange membranes, Desalination 122 (1999) 53–62.
[15] M. Hichour, F. Persin, J. Sandeaux, C. Gavach, Fluoride removal from waters by Donnan dialysis, Sep. Purif. Technol. 18 (1999) 1–11.
[16] H. Lounici, L. Addour, D. Belhocine, H. Grib, S. Nicolas, B. Bariou, N. Mameri, Study of a new technique for fluoride removal from water, Desalination 114 (1997) 241–251.
[17] S.K. Adhikary, U.K. Tipnis, W.P. Harkare, K.P. Govindan, Defluoridation during desalination of brackish water by electrodialysis, Desalination 71 (1989) 301–312.
[18] S. Saha, Treatment of aqueous effluent for fluoride removal, Water Res. 27 (1993) 1347–1350.

[19] Y.H. Li, S. Wang, X. Zhang, J. Wei, C. Xu, Z. Luan, D. Wu, Adsorption of fluoride from water by aligned carbon nanotubes, Mater. Res. Bull. 38 (2003) 469–476.
[20] R.Q. Long, R.T. Yang, Carbon nanotubes as superior sorbent for dioxin removal, J. Am. Chem. Soc. 123 (2001) 2058–2059.
[21] Y.H. Li, S. Wang, A. Cao, D. Zhao, X. Zhang, C. Xu, Z. Luan, D. Ruan, J. Liang, D. Wu, B. Wei, Adsorption of fluoride from water by amorphous alumina supported on carbon nanotubes, Chem. Phys. Lett. 350 (2001) 412–416.
[22] Y.H. Li, S. Wang, J. Wei, X. Zhang, C. Xu, Z. Luan, D. Wu, B. Wei, Lead adsorption on carbon nanotubes, Chem. Phys. Lett. 357 (2002) 263–266.
[23] Y.H. Li, S. Wang, Z. Luan, J. Ding, C. Xu, D. Wu, Adsorption of cadmium(II) from aqueous solution by surface oxidized carbon nanotubes, Carbon 41 (2003) 1057–1062.
[24] T. Mohammadi, M. Ahmadzadeh Tofighy, A. Pak, Synthesis of carbon nanotubes on macroporous kaolin substrate via a new simple CVD method, Int. J. Chem. React. Eng. 7 (2009) A75.
[25] H.J. Ahn, J.H. Lee, Y. Jeong, J.H. Lee, C.S. Chi, H.J. Oh, Nanostructured carbon cloth electrode for desalination from aqueous solutions, Mater. Sci. Eng. A 449–451 (2007) 841–845.
[26] I.I. Salame, T.J. Bandosz, Role of surface chemistry in adsorption of phenol on activated carbons, J. Colloid Interface Sci. 264 (2003) 307–312.
[27] J. Rivera-Utrilla, I. Bautista-Toledo, M.A. Ferro-Garcia, C. Moreno-Castilla, Activated carbon surface modifications by adsorption of bacteria and their effect on aqueous lead adsorption, J. Chem. Technol. Biotechnol. 76 (2001) 1209–1215.
[28] H. Faghihian, M. Kooravand, H. Atarodi, Synthesis of a novel carbon nanofiber structure for removal of lead, Korean J. Chem. Eng. 30 (2013) 357–363.
[29] X. Xia, X. Zeng, J. Liu, W. Xu, Preparation and characterization of epoxy/kaolinite nanocomposites, J. Appl. Polym. Sci. 118 (2010) 2461–2466.
[30] L. Vaculikova, E. Plevova, S. Vallova, I. Koutnik, Characterization and differentiation of kaolinites from selected Czech deposits using infrared spectroscopy and differential thermal analysis, Acta Geodyn. Geomater. 8 (2011) 59–67.
[31] X. Liu, M. Wang, S. Zhang, B. Pan, Application potential of carbon nanotubes in water treatment: A review, J. Environ. Sci. 25 (2013) 1263–1280.
[32] P. Liang, Q. Ding, F. Song, Application of multiwalled carbon nanotubes as solid phase extraction sorbent for preconcentration of trace copper in water samples, J. Sep. Sci. 28 (2005) 2339–2343.
[33] P.X. Hou, C. Liu, H.M. Cheng, Purification of carbon nanotubes, Carbon 46 (2008) 2003–2025.
[34] J. Liu, A.G. Rinzler, H. Dai, J.H. Hafner, R.K. Bradley, P.J. Boul, A. Lu, T. Iverson, K. Shelimov, C.B. Huffman, F. Rodriguez-Macias, Y.S. Shon, T.R. Lee, D.T. Colbert, R.E. Smalley, Fullerene pipes, Science 280 (1998) 1253–1256.
[35] D. Eom, D. Prezzi, K.T. Rim, H. Zhou, M. Lefenfeld, S. Xiao, C. Nuckolls, M.S. Hybertsen, T.F. Heinz, G.W. Flynn, Structure and electronic properties of graphene nanoislands on Co (0001), Nano Lett. 9 (2009) 2844–2848.
[36] Y. Li, P. Zhang, Q. Du, X. Peng, T. Liu, Z. Wang, Y. Xia, W. Zhang, K. Wang, H. Zhu, D. Wu, Adsorption of fluoride from aqueous solution by graphene, J. Colloid Interface Sci. 363 (2011) 348–354.
[37] Y.S. Ho, G. McKay, The kinetics of sorption of divalent metal ions onto sphagnum moss peat, Water Res. 34 (2000) 735–742.
[38] Y.S. Ho, G. McKay, Pseudo-second order model for sorption processes, Process Biochem. 34 (1999) 451–465.
[39] W.J. Weber, J.C. Morris, Kinetics of adsorption on carbon from solution, J. Sanit. Eng. Div. Am. Soc. Civ. Eng. 89 (1963) 31–60.
[40] P. Satish, R. Sameer, P. Naseema, Defluoridation of water using biosorbents: Kinetic and thermodynamic study, Int. J. Res. Chem. Environ. 3 (2013) 125–135.